

The Silicon Vertex Detector of the Belle II experiment

2 **A.B. Kaliyar**,^{a,*} **K. Adamczyk**,^b **L. Aggarwal**,^c **H. Aihara**,^d **T. Aziz**,^e **S. Bacher**,^b
 3 **S. Bahinipati**,^f **G. Batignani**,^{g,h} **J. Baudot**,ⁱ **P. K. Behera**,^j **S. Bettarini**,^{g,h} **T. Bilka**,^k
 4 **A. Bozek**,^b **F. Buchsteiner**,^a **G. Casarosa**,^{g,h} **L. Corona**,^h **S. B. Das**,^l **G. Dujany**,ⁱ
 5 **C. Finck**,ⁱ **F. Forti**,^{g,h} **M. Friedl**,^a **A. Gabrielli**,^{m,n} **B. Gobbo**,ⁿ **S. Halder**,^e **K. Hara**,^{o,p}
 6 **S. Hazra**,^e **T. Higuchi**,^q **C. Irmler**,^a **A. Ishikawa**,^{o,p} **Y. Jin**,ⁿ **M. Kaleta**,^b **J. Kandra**,^k
 7 **K. H. Kang**,^q **P. Kodyš**,^k **T. Kohriki**,^o **R. Kumar**,^r **K. Lalwani**,^l **K. Lautenbach**,^t
 8 **R. Leboucher**,^t **S. C. Lee**,^s **J. Libby**,^j **L. Martel**,ⁱ **L. Massaccesi**,^{g,h} **G. B. Mohanty**,^e
 9 **S. Mondal**,^{g,h} **K. R. Nakamura**,^{o,p} **Z. Natkaniec**,^b **Y. Onuki**,^d **F. Otani**,^q
 10 **A. Paladino**,^{A, g,h} **E. Paoloni**,^{g,h} **H. Park**,^s **L. Polat**,^t **K. K. Rao**,^e **I. Ripp-Baudot**,ⁱ
 11 **G. Rizzo**,^{g,h} **Y. Sato**,^o **C. Schwanda**,^a **J. Serrano**,^t **T. Shimasaki**,^q **J. Suzuki**,^o
 12 **S. Tanaka**,^{o,p} **H. Tanigawa**,^d **F. Tenchini**,^{g,h} **R. Thalmeier**,^a **R. Tiwary**,^e
 13 **T. Tsuboyama**,^o **Y. Uematsu**,^d **L. Vitale**,^{m,n} **Z. Wang**,^d **J. Webb**,^u **O. Werbycka**,ⁿ
 14 **J. Wiechczynski**,^b **H. Yin**^a and **L. Zani**^{B,t}

15 ^a*Institute of High Energy Physics, Austrian Academy of Sciences, 1050 Vienna, Austria*

16 ^b*H. Niewodniczanski Institute of Nuclear Physics, Krakow 31-342, Poland*

17 ^c*Punjab University, Chandigarh 160014, India*

18 ^d*Department of Physics, University of Tokyo, Tokyo 113-0033, Japan*

19 ^e*Tata Institute of Fundamental Research, Mumbai 400005, India*

20 ^f*Indian Institute of Technology Bhubaneswar, Bhubaneswar 752050, India*

21 ^g*Dipartimento di Fisica, Università di Pisa, I-56127 Pisa, Italy, ^Apresently at INFN Sezione di Bologna,*
 22 *I-40127 Bologna, Italy*

23 ^h*INFN Sezione di Pisa, I-56127 Pisa, Italy*

24 ⁱ*IPHC, UMR 7178, Université de Strasbourg, CNRS, 67037 Strasbourg, France*

25 ^j*Indian Institute of Technology Madras, Chennai 600036, India*

26 ^k*Faculty of Mathematics and Physics, Charles University, 121 16 Prague, Czech Republic*

27 ^l*Malaviya National Institute of Technology Jaipur, Jaipur 302017, India*

28 ^m*Dipartimento di Fisica, Università di Trieste, I-34127 Trieste, Italy*

29 ⁿ*INFN Sezione di Trieste, I-34127 Trieste, Italy*

30 ^o*High Energy Accelerator Research Organization (KEK), Tsukuba 305-0801, Japan*

31 ^p*The Graduate University for Advanced Studies (SOKENDAI), Hayama 240-0193, Japan*

32 ^q*Kavli Institute for the Physics and Mathematics of the Universe, University of Tokyo, Kashiwa 277-8583,*
 33 *Japan*

34 ^r*Punjab Agricultural University, Ludhiana 141004, India*

35 ^s*Department of Physics, Kyungpook National University, Daegu 41566, Korea*

*Speaker

³⁶ ¹*Aix Marseille Université , CNRS/IN2P3, CPPM, 13288 Marseille, France,* ^B*presently at INFN Sezione di*
³⁷ *Roma Tre, I-00185 Roma, Italy*

³⁸ ⁴*School of Physics, University of Melbourne, Melbourne, Victoria 3010, Australia*

³⁹ *E-mail: abdulbasith.kaliyar@oeaw.ac.at*

⁴⁰ The Belle II silicon vertex detector (SVD) is a four-layer double-sided silicon strip detector installed within the Belle II detector located at KEK, Japan. The SVD has been operating smoothly and reliably since the start of data taking in March 2019. The data quality and radiation damage effects have been continuously monitored. In this article, we report the operational experience of SVD, reconstruction performance, and effects of beam background and radiation damage. We also discuss some of the recent efforts to improve the software robustness targeting the high luminosity scenario and hardware activities performed during the first long shutdown of the Belle II experiment.

1. Introduction

The Belle II experiment [1] aims to make precise measurements of weak-interaction parameters, study exotic hadrons, and search for physics beyond the Standard Model. The experiment is currently underway at the SuperKEKB accelerator research center located in Tsukuba, Japan. SuperKEKB [2] is an asymmetric-energy e^+e^- (4 GeV on 7 GeV) collider that operates at centre-of-mass energies near the $\Upsilon(4S)$ resonance (10.58 GeV). The peak luminosity achieved so far is $4.7 \times 10^{34} \text{ cm}^{-2}\text{s}^{-1}$, which is the current world record. The ultimate target is to reach a peak luminosity of $6 \times 10^{35} \text{ cm}^{-2}\text{s}^{-1}$. The Belle II detector, located around the collider interaction point, has so far collected 426 fb^{-1} of data. The eventual goal is to record 50 ab^{-1} of data in the next decade.

The vertex detector (VXD) is the innermost component in the Belle II detector system located closest to the interaction point. Comprising six layers, it includes two inner layers of silicon pixel detectors (PXD) [3], based on depleted field effect transistor sensors, and four outer layers of silicon strip detectors, known as the silicon vertex detector (SVD) [4]. The SVD is crucial for extrapolating the measured tracks to the PXD that point at a region of interest, which helps to significantly reduce the amount of data recorded by the PXD. Besides that, the SVD performs standalone tracking of low-momentum particles, vertex detection of K_S^0 and Λ particles, as well as contributes to the charged-particle identification by providing energy-loss information.

In July 2022, Belle II temporarily paused operation for the first long shutdown to allow accelerator maintenance and improvements to the detector. The VXD was reinstalled during this time with a new complete PXD and the same SVD. In this article, we present a detailed description of the SVD, its performance until July 2022, effects of radiation damage, the software improvements aimed towards high-luminosity running, and finally a report on the the VXD reinstallation and commissioning during the long shutdown.

2. The Belle II Silicon Vertex Detector

The Belle II SVD is composed of four layers of double-sided silicon strip detectors (DSSD), namely layers 3, 4, 5, and 6, placed at radii of 39, 80, 104, and 135 mm, respectively, from the beam pipe. The material budget is about 0.7% of radiation length X_0 per layer. In total, there are 172 DSSD sensors representing an area of 1.2 m^2 and 224,000 readout strips. There are three types of DSSDs: small rectangular sensors in layer 3, large rectangular sensors in the barrel region of layers 4, 5, and 6, and slanted trapezoidal sensors to extend spatial coverage toward the forward region of these three outermost layers. The readout strips are AC coupled and there is one intermediate floating strip between two readout implants. The full depletion voltage ranges from 20 to 60 V, and the operating voltage is 100 V. The radiation hardness of SVD sensors is about 6 Mrad.

The SVD uses the APV25 [5] frontend readout ASIC, which has 128 input channels. It collects signals from the strips and provides an analog readout. APV25 has a fast 50 ns shaping time and a radiation hardness of up to 100 Mrad. By default, the chip operates in multipeak mode at a clock frequency of 31.8 MHz, which is 1/8th of the SuperKEKB bunch-crossing frequency.

79 3. Operation and performance

80 The SVD has been operating smoothly and reliably since its installation in 2019. The total
 81 fraction of masked strips due to defects is less than 1% and only one out of 1748 APV25s was
 82 temporarily disabled. Temperature and calibration constants are evolving within the expected ranges
 83 due to radiation damage. The hit efficiency exceeds 99% for all the sensors. Figure 1 shows the
 84 distributions of signal cluster charge and cluster signal-to-noise ratio (SNR) of an example sensor
 85 measured in 2022 and 2020. The signal cluster charge is normalized to the track path length in the
 86 silicon to correct for the track’s incidence angle. The normalized cluster charge is found to be in
 87 good agreement with expectations and similar across all sensors. The charge matches the expected
 88 minimum ionizing particle value of $24000 e^-$ within 15%, which is the uncertainty in the absolute
 89 APV25 gain calibration. We define the cluster SNR by dividing the total cluster charge by the
 90 quadratic sum of the noise values from each strip in the cluster. A small decrease in cluster SNR
 91 is observed in the 2022 data due to approximately 20–30% increased noise from radiation damage.
 92 All 172 DSSD sensors generally exhibit very good SNR, with most probable values typically falling
 93 within the range of 13 to 30, depending on sensor side and position.

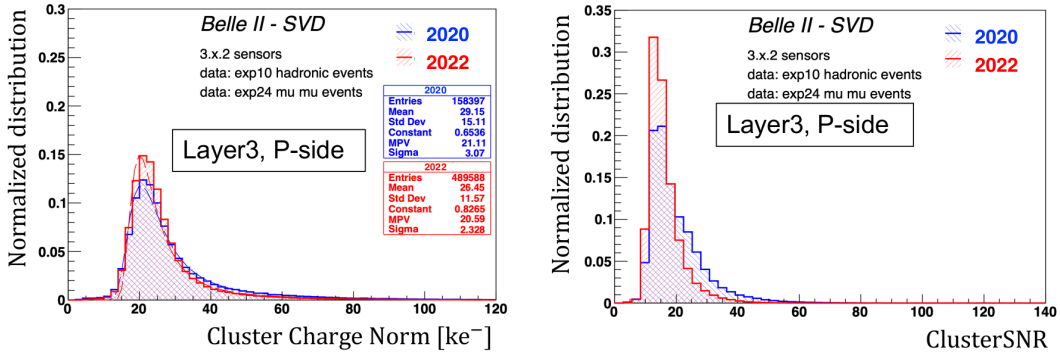


Figure 1: Distributions of signal cluster charge (left) and cluster SNR (right) for P-strips of a layer 3 sensor.

94 The cluster-position resolution is crucial for vertexing and track reconstruction performance.
 95 The position resolution of the SVD is estimated from the residual between the cluster position and the
 96 unbiased track extrapolation, after subtracting quadratically the track extrapolation uncertainty [6].
 97 Studies based on $e^+e^- \rightarrow \mu^+\mu^-$ events show a resolution of 7–12 μm for the P-side and 15–25 μm
 98 for the N-side. These are in fair agreement with expectations from the sensor pitch. Good stability
 99 of position resolution over time is also confirmed by comparing measurements from 2022 with
 100 those from 2020.

101 The SVD also offers excellent hit-time resolution. It is measured from the residuals between
 102 the hit time and the e^+e^- collision time provided by the central drift chamber of the Belle II detector.
 103 The measured hit-time resolution is 2.9 ns (2.4 ns) for the P (N) side. The hit-time information
 104 is also used to mitigate the machine-related background, which is typically unassociated with the
 105 e^+e^- collisions. This off-time-hit background enters the triggered-data acquisition window and
 106 increases the strip occupancy. Background occupancy above a certain threshold may cause tracking

107 performance degradation. In the case of multiple particles crossing the sensor, we can use the time
108 difference between the P- and N- side clusters to suppress the wrong combination of these clusters.
109 By requiring the cluster time within 50 ns of the event time and time difference between the P- and
110 N-side clusters within 20 ns, 50% of the off-time background hits can be rejected while maintaining
111 99% tracking efficiency. This allows us to set the hit-occupancy limit of layer 3 to 4.7% without
112 tracking performance deterioration.

113 We are currently developing two new algorithms that utilize the SVD time information to
114 further relax the hit-occupancy limit and enhance offline software robustness in the high-background
115 environment. One of these algorithms requires a selection of the tracktime, which is computed by
116 combining the hit-time of SVD clusters associated with a track. This reduces the fake-track rate, thus
117 relaxing the hit-occupancy limit. The second algorithm involves grouping SVD clusters based on
118 the hit-time information. The cluster-time distribution has a clear grouping structure since clusters
119 from different bunches are collected within the acquisition time window of the triggered event.
120 While signal clusters are grouped around the event time, background hits, caused by neighboring
121 beam-bunches, form other groups. The inclusion of these two algorithms allow us to set the
122 hit-occupancy limit at around 6%. Further software improvement and optimization are currently
123 ongoing before incorporating these features into the actual data processing.

124 **4. Beam background and radiation effects**

125 In this section, we discuss the impact of radiation damage on the SVD sensors during their
126 operation. The beam-induced background increases the hit occupancy and causes radiation damage
127 to the sensors. The radiation damage can affect the strip noise, leakage current, and full depletion
128 voltage of sensors, so these quantities are constantly monitored during the operation. The current
129 average hit occupancy on layer 3 sensors is less than 0.5% which is a level that does not affect
130 tracking performance. We estimate the radiation dose in the SVD using the data from diamond
131 sensors mounted on the beam pipe and the bellows pipes outside the VXD. The total integrated
132 radiation dose on layer 3 sensors is 70 krad, which corresponds to an equivalent 1 – MeV neutron
133 fluence of 1.6×10^{11} n_{eq}/cm², assuming the ratio of a neutron fluence to a radiation dose of
134 2.3×10^9 n_{eq}/cm²/krad based on Monte-Carlo simulation.

135 During the operation, the strip noise, dominated by the interstrip capacitance, increases by
136 about 20% (30%) for the N-side (P-side) and is expected to be saturated. The leakage current is
137 gradually increasing; in general, its value shows a linear dependence on the accumulated dose, as
138 expected from the non-ionising energy-loss model [7]. So far, this increase has had a negligible
139 contribution to the noise because of the small leakage-current and short APV25 shaping time.
140 However, after 6 Mrad, the leakage current contribution to the noise might become significant
141 which can reduce the SNR below 10 in layer 3. So far no changes in full depletion voltage have
142 been observed in the operating sensors.

143 **5. VXD reinstallation during first long shutdown**

144 In July 2022, Belle II paused its operation for the first long shutdown to allow accelerator
145 maintenance and implement upgrades to the detector. We installed a brand new pixel detector

146 (PXD2) in the VXD volume, with a complete second layer, alongside the current SVD. The SVD
147 crew engaged in intense hardware activities during the deinstallation and reinstallation of the VXD.
148 On May 10, 2023, the VXD was safely extracted from the Belle II detector, followed by dismounting
149 the two SVD half-shells from the old PXD and mounting them on the PXD2. All these delicate
150 operations involved several steps with extensive testing of the detector and the environmental
151 monitoring system, to check the performance of the system after each step. The healthiness of all
152 SVD sensors was confirmed during the commissioning of the new VXD in the clean room. In
153 July 2023, the new VXD was successfully reinstalled into the Belle II detector. Additional tests,
154 including cosmic-ray runs, were performed before the start of the actual beam operation. After this
155 shutdown, Belle II officially restarted data taking in January 2024, and so far, SVD is performing
156 as smoothly as before.

157 6. Conclusion

158 The Belle II SVD has been taking high-quality data since March 2019. Operation is stable
159 and reliable, with excellent detector performance. Effects from radiation damage are observed at
160 the expected level; however, their contribution has not caused any degradation of the SVD tracking
161 performance so far. During the first long shutdown, a new VXD was successfully reinstalled into
162 the Belle II detector, incorporating the new PXD2 together with the existing SVD.

163 7. Acknowledgements

164 This project has received funding from the European Union's Horizon 2020 research and
165 innovation programme under the Marie Skłodowska-Curie grant agreements No 644294, 822070
166 and 101026516 and ERC grant agreement No 819127. This work is supported by MEXT, WPI
167 and JSPS (Japan); ARC (Australia); BMBWF (Austria); MSMT (Czechia); CNRS/IN2P3 (France);
168 AIDA-2020 (Germany); DAE and DST (India); INFN (Italy); NRF and RSRI (Korea); and MNiSW
169 (Poland).

170 References

- 171 [1] T. Abe *et al.*, (Belle-II Collaboration), Belle II Technical Design Report [[arXiv:1011.0352](https://arxiv.org/abs/1011.0352)].
- 172 [2] Y. Ohnishi *et al.*, Prog. Theor. Exp. Phys. **2013**, 03A011 (2013).
- 173 [3] B. Wang *et al.*, (Belle-II DEPFET and PXD Collaborations), Nucl. Instrum. Meth. A **1032**,
174 166631 (2022).
- 175 [4] K. Adamczyk *et al.*, (Belle-II SVD Collaboration) JINST **17**, P11042 (2022).
- 176 [5] M. J. French *et al.*, Nucl. Instrum. Meth. A **466**, 359 (2001).
- 177 [6] R. Leboucher *et al.*, Nucl. Instrum. Meth. A **1033**, 166746 (2022).
- 178 [7] G. Lindström *et al.*, Nucl. Instrum. Meth. A **465**, 60 (2001).